AD-A124 036 ANALYSIS OF LAYERED COMPOSITE PLATES BY THREE-DIMENSIONAL ELASTICITY THEORY(U) OKLAHOMA UNIV NORMAN J N REDDY ET AL. NOV 82 TR-31 N00014-78-C-0647 1/1

UNCLASSIFIED F/G 11/4 NL

END
DATE
FILMED
2 83
DTIC

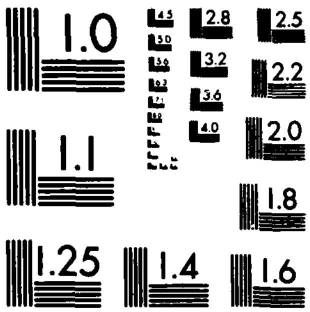


MICROCOPY RESOLUTION TEST CHART
NATIONAL BUREAU OF STANDARDS-1963-A

Department of the Navy
OFFICE OF NAVAL RESEARCH
Mechanics Division
Arlington, Virginia 22217

Grant N00014-78-C-0647
Project NR 064-609
Technical Report No. 31

(12)

Report VPI-E-82-31

# ANALYSIS OF LAYERED COMPOSITE PLATES BY THREE-DIMENSIONAL ELASTICITY THEORY

J. N. Reddy and T. Kuppusamy
Virginia Polytechnic Institute and State University
Blacksburg, VA 24061



November 1982

## ANALYSIS OF LAYERED COMPOSITE PLATES BY THREE-DIMENSIONAL ELASTICITY THEORY


Abstract

This report contains two parts: the first part is concerned with the natural vibrations of laminated anisotropic plates, and the second part is concerned with geometrically nonlinear, finite-element analysis of the bending of cross-ply laminated anisotropic composite plates. Individual laminae are assumed to be homogeneous, orthotropic and linearly elastic. A fully three-dimensional isoparametric finite element with eight nodes (i.e., linear element) and 24 degrees of freedom (three displacement components per node) is used to model the laminated plate. The finite element results of the linear analysis are found to agree very well with the exact solutions of cross-ply laminated rectangular plates under sinusoidal loading. The finite element results of the three-dimensional, geometrically nonlinear analysis are compared with those obtained by using a shear deformable, geometrically nonlinear, plate theory. It is found that the deflections predicted by the shear deformable plate theory are in fair agreement with those predicted by 3-D elasticity theory; however, stresses are found to be not in good agreement. The results of natural vibration indicate that for relatively thick plates, the shear deformable plate theory predicts frequencies higher than those predicted by the 3-D theory.

Department of the Navy
OFFICE OF NAVAL RESEARCH
Mechanics Division
Arlington, Virginia 22217

Grant N00014-78-C-0647
Project NR 064-609
Technical Report No. 31

Report VPI-E-82.31

# ANALYSIS OF LAYERED COMPOSITE PLATES BY THREE-DIMENSIONAL ELASTICITY THEORY

J. N. Reddy and T. Kuppusamy
Virginia Polytechnic Institute and State University
Blacksburg, VA 24061

November 1982

# NATURAL VIBRATIONS OF LAMINATED ANISOTROPIC PLATES USING 3D-ELASTICITY THEORY

J. N. Reddy
Department of Engineering Science and Mechanics

and

T. Kuppusamy
Department of Civil Engineering

Virginia Polytechnic Institute and State University
Blacksburg, VA 24061

## ABSTRACT

The paper contains a description of the three-dimensional elasticity equations and the associated finite element model for natural vibrations of laminated rectangular plates. The numerical results for natural frequencies are compared with those obtained by a shear deformable plate theory. A number of cross-ply and angle-ply rectangular plates are analyzed for natural frequencies. For relatively thick plates, the plate element predicts frequencies higher than those predicted by the 3-D element.

## INTRODUCTION

The present study is motivated by the lack of three-dimensional finite-element results for natural frequencies of laminated composite plates. For relatively thick plates (i.e., for side-to-thickness ratios less than 10), the classical plate theory and certain thick plate theories predict higher frequencies, and therefore it is of interest to have a 3-D finite element to accurately predict natural frequencies. The following literature provides the background for the present study.

The shear deformable plate theory (see Reissner [1] and Mindlin [2]) is a twc-dimensional theory derived from the assumption that the strains $\varepsilon_z$, $\varepsilon_{xz}$, and $\varepsilon_{yz}$ are independent of z, which leads to the displacement field of the form

$$\begin{aligned} u &= u_o(x,y) + z\phi_x(x,y) \\ v &= v_o(x,y) + z\phi_y(x,y) \\ w &= w_o(x,y). \end{aligned} \tag{1}$$

Here $u_0$, $v_0$, and $w_0$ denote the displacements along x, y, and z directions respectively of a point located on the midplane of the plate, which coincides with the xy-plane of the coordinate system; $\phi_x$ and $\phi_y$ denote the rotations (taken clockwise positive) of a line element, initially perpendicular to the midplane, about y and x axes, respectively. The classical plate theory is a special case (derived from the assumption that $\varepsilon_z = \varepsilon_{xz} = \varepsilon_{yz} = 0$) of the shear deformable plate theory in which the transverse shear strains are assumed to be zero:

$$\phi_x = -\frac{\partial w_o}{\partial x} \quad , \quad \phi_y = -\frac{\partial w_o}{\partial y}. \tag{2}$$

The classical plate theory is based on the Kirchoff-Love assumption that planes initially normal to the midplane remain plane and normal to the midsurface after bending, i.e., equivalently, conditions in Eq. (2) hold.

The first lamination thin plate theory is due to Reissner and Stavsky [3]. An extension of the thick plate theory to arbitrarily laminated anisotropic plates was presented by Yang, Norris, and Stavsky [4]. Whitney and Pagano [5], and Reddy and Chao [6] presented exact solutions of the theory when applied to laminated rectangular plates under certain lamination schemes, boundary conditions, and sinusoidal distribution of transverse loads. Reddy and his colleagues [7-12] presented finite-element analyses of the bending, vibration and transient response of laminated anisotropic composite plates.

The three-dimensional lamination theory is based on the assumption that the individual lamina behave according to the 3-D elasticity theory. At the interfaces of individual lamina, the displacements are assumed to be continuous. Dana and Barker [13] used the cubic isoparametric brick element and Putcha and Reddy [14] used the linear brick element to investigate the bending of layered plates. Recently, Kuppusamy and Reddy [15] used the linear isoparametric brick element to study the geometrically nonlinear behavior of laminated plates. The present study is concerned with the application of the linear brick element to the natural vibration of laminated composite plates.

## GOVERNING EQUATIONS

Consider a plate arbitrarily laminated of a finite number of orthotropic layers of uniform thickness. The equations of motion of a three-dimensional elastic continuum under the assumption of

infinitesimal strains, in the Lagrangian description, are given by

$$\sum_{j=1}^{3} \frac{\partial \sigma_{ij}^{(k)}}{\partial x_j} = \rho^{(k)} \frac{\partial^2 u_i^{(k)}}{\partial t^2} \quad , \quad i = 1,2,3, \tag{3}$$

where $\sigma_{ij}^{(k)} = \sigma_{ji}^{(k)}$ denote the components of the Cauchy stress tensor, $\rho^{(k)}$ is the density, and $u_i^{(k)}$ are the displacement components of the k-th layer. All of the variables are referred to the plate coordinates $x_i$. It is assumed that there are no body forces in the problem. At the interface of two layers it is assumed that the displacements are continuous.

$$u_i^{(k)} = u_i^{(k+1)}. \tag{4}$$

The strain-displacement relations are given by

$$\varepsilon_{ij} = \frac{1}{2} \left(\frac{\partial u_i}{\partial x_j} + \frac{\partial u_j}{\partial x_i}\right) \quad , \quad i,j = 1,2,3. \tag{5}$$

The stress-strain relations, for individual lamina, in the plate coordinates are given by

$$\sigma_i^{(k)} = \sum_{j=1}^{6} c_{ij}^{(k)} \varepsilon_j^{(k)} \quad , \quad i = 1,2,\ldots,6, \tag{6}$$

where

$$\begin{aligned} &\sigma_1 = \sigma_{11},\ \sigma_2 = \sigma_{22},\ \sigma_3 = \sigma_{33},\ \sigma_4 = \sigma_{23},\ \sigma_5 = \sigma_{13},\ \sigma_6 = \sigma_{12}, \\ &\varepsilon_1 = \varepsilon_{11},\ \varepsilon_2 = \varepsilon_{22},\ \varepsilon_3 = \varepsilon_{33},\ \varepsilon_4 = 2\varepsilon_{23},\ \varepsilon_5 = 2\varepsilon_{13},\ \varepsilon_6 = 2\varepsilon_{12}, \end{aligned} \tag{7}$$

and $c_{ij}^{(k)}$ are the material stiffnesses of k-th layer referred to the plate coordinates.

Equations (2), (3), and (6) are to be solved using appropriate boundary conditions. At a point on the boundary of the plate, one should specify:

$$\begin{aligned} &\text{either } u_i = \hat{u}_i \quad (i = 1,2,3), \\ &\text{or} \quad n_j \sigma_{ij} = \hat{t}_i \quad (i = 1,2,3), \end{aligned} \tag{8}$$

where $n_j$ denotes the j-th component the unit outward normal $\hat{n}$ to the boundary, and $\hat{u}_i$ and $\hat{t}_i$ denote specified values of the displacement and traction components.

## FINITE-ELEMENT MODEL

The variational formulation of Eqs. (2), (3), and (6), over a typical element $\Omega^e$, is given by

$$0 = \int_{\Omega^e} (\delta u_{i,j}\sigma_{ij} + \rho\delta u_i \frac{\partial^2 u_i}{\partial t^2})\, dxdydz - \int_{\Gamma^e} n_j\sigma_{ij}t_i ds \tag{9}$$

where $\delta$ denotes the variational symbol. Let $u_i$ be interpolated over the element $\Omega^e$ by

$$u_i = \sum_{\alpha=1}^{8} u_i^\alpha \phi_\alpha \quad (i = 1,2,3) \tag{10}$$

where $\phi_\alpha(x,y,z)$ denote the trilinear interpolation functions of the eight-node isoparametric brick element, and $u_i^\alpha(t)$ denote the value of $u_i$ at node $\alpha$ and time t. Substitution of Eq. (10) into Eq. (9), we obtain

$$\begin{bmatrix} [M^{11}] & [M^{12}] & [M^{13}] \\ & [M^{22}] & [M^{23}] \\ \text{symm.} & & [M^{33}] \end{bmatrix} \begin{Bmatrix} \{\ddot{u}_1\} \\ \{\ddot{u}_2\} \\ \{\ddot{u}_3\} \end{Bmatrix} + \begin{bmatrix} [K^{11}] & [K^{12}] & [K^{13}] \\ & [K^{22}] & [K^{23}] \\ \text{symm.} & & [K^{33}] \end{bmatrix} \begin{Bmatrix} \{u_1\} \\ \{u_2\} \\ \{u_3\} \end{Bmatrix}$$

$$= \begin{Bmatrix} \{F_1\} \\ \{F_2\} \\ \{F_3\} \end{Bmatrix} \qquad (11)$$

where $[K^{ij}]$ and $[M^{ij}]$ are coefficient matrices associated with vector $\{u_j\}$ in the i-th equation. For the sake of brevity the explicit form of the coefficients is not given here. The mass and bending coefficients are to be evaluated using full integration and the shear coefficients (in [K]) are to be evaluated using the reduced integration.

To investigate the free vibration, we set $\{F_i\} = \{0\}$, and

$$u_i^\alpha = u_{io}^\alpha e^{p\omega t} \quad (i = 1,2,3;\ \alpha = 1,2,\ldots,8) \qquad (12)$$

where $p = \sqrt{-1}$ and $\omega$ denotes the frequency of natural vibration. Substitution of Eq. (12) into Eq. (11) gives the following generalized eigenvalue problem:

$$([K] - \omega^2[M])\{\Delta\} = \{0\}, \qquad (13)$$

where $\{\Delta\} = \{\{u_{10}\}, \{u_{20}\}, \{u_{30}\}\}^T$. Equations (13) are assembled in the usual manner, and (homogeneous) boundary conditions are imposed before solving the eigenvalue problem by any standard eigenvalue program.

## NUMERICAL RESULTS

In all of the examples considered here, the biaxial symmetry is exploited to model only one quadrant of the plate. The quadrant is modeled using 4 x 4 x n mesh of the eight-node brick elements. Here n denotes the number of layers in the plate. The following two types of high-modulus composite materials are used in the present study:

Material I: $E_1/E_2=25$, $E_3/E_2=1$, $G_{12}/E_2=G_{13}/E_2=0.5$, $G_{23}/E_2=0.2$

$$\nu_{12}=\nu_{13}=\nu_{23}=0.25,\ \rho=1.0$$

$$\text{Material II: } E_1/E_2=40,\ E_3/E_2=1,\ G_{12}/E_2=G_{13}/E_2=0.6,\ G_{23}/E_2=0.2$$
$$\nu_{12}=\nu_{13}=\nu_{23}=0.25,\ \rho=1.0. \qquad (14)$$

A value of 5/6 is used for the shear correction coefficient, $K_i^2$. The boundary conditions used in the present study are shown in Fig. 1.

The first example is concerned with three-layer cross-ply square plates: 0°/90°/0°, $h_1 = h_3 = h/4$, $h_2 = h/2$. This is also equivalent to four-layer cross-ply (0°/90°/90°/0°) laminate made of equal thickness layers. Table 1 contains a comparison of the fundamental frequencies obtained by the plate theory [6] and the present 3-D elasticity theory. It is clear from the results that the solutions predicted by the shear deformable plate theory are higher than those predicted by the 3-Delasticity theory; of course, the classical thin plate theory predicts even higher frequencies. The difference can be explained as follows: in plate theories, the transverse shear strains and normal strains are either completely neglected (like in the classical plate theory) or included in an approximate sense (e.g., the transverse shear strains are included in the shear deformable plate theory). Consequently, the modeled plate is stiffer than the actual one. Due to the lower value of the shear modulus relative to the in-plane Young's moduli, the transverse shear deformation effects are more pronounced in composite plates. In the 3-D theory, no assumption is made to neglect the shear or normal strains, and therefore the frequencies predicted are more accurate (and realistic). For large ratios of side to thickness, the transverse shear strains and normal strains are negligible and therefore both theories predict almost the same frequencies. It is also clear from the results presented in Table 1 that the degree of material

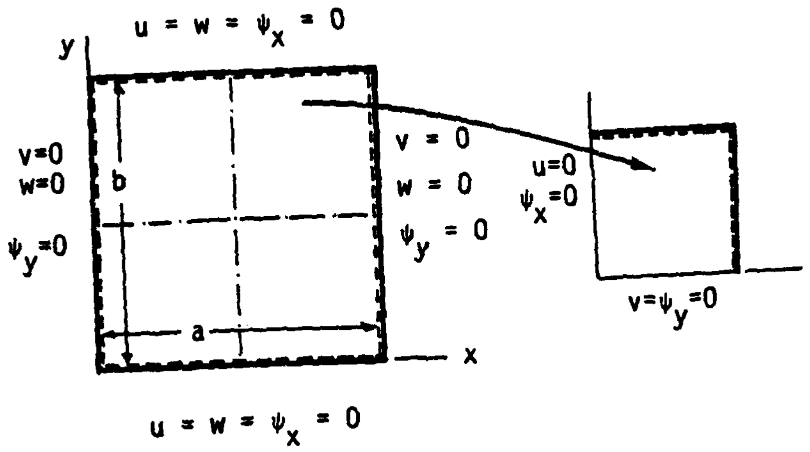


(a) Boundary conditions for cross-ply plates(BC1)

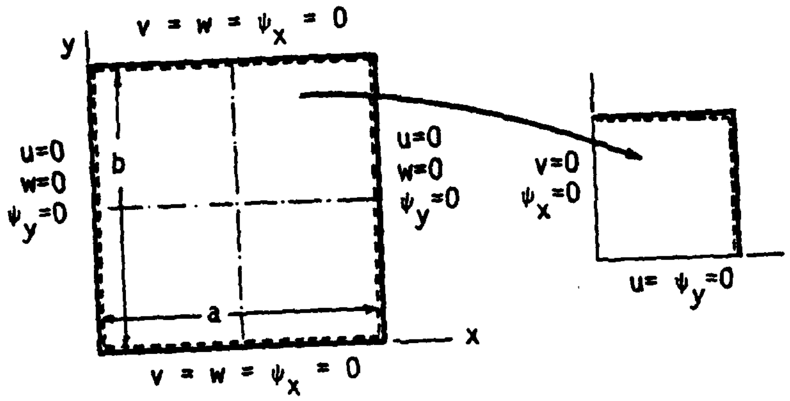


(b) Boundary conditions for angle-ply plates (BC2)

Figure 1 Boundary conditions used in the present study for cross-ply and angle-ply plates

anisotropy as well as plate aspect ratio adversely affect the accuracy of the frequencies predicted by the plate theory.

The second example is concerned with the vibration of a square sandwich plate. The material of the face sheets is the same as Material I, and that of the core is transversely isotropic with the following properties:

$$E_1/E_2 = 1.0,\ E_3/E_2 = 12.5,\ \rho = 1.0$$
$$G_{13} = G_{23} = 1.5E_2,\ G_{12} = 0.4E_2$$
$$\nu_{12} = 0.25,\ \nu_{13} = \nu_{23} = 0.02. \tag{15}$$

The thickness of each face sheet is 0.1h and that of the core is 0.8h. Table 2 contains the nondimensionalized frequencies obtained using the 3-D elasticity theory. These results should serve as bench marks for future comparisons.

Table 3 contains nondimensionalized natural frequencies of two-layer cross-ply (0°/90°) and angle-ply (45°/-45°) square plates. From the results presented in Table 3 and 4, it follows that two-layer cross-ply plates have lower frequencies than both two-layer angle-ply plates and four-layer cross-ply (0°/90°/90°/0°) plates (of equal thickness layers). On the other hand, the two-layer angle-ply plates have higher frequencies than the cross-ply plates analyzed here. These observations indicate that the two-layer cross-ply laminates are structurally more flexible whereas the two-layer angle-ply laminates are more stiffer than the four-layer (0°/90°/90°/0°) cross-ply plates.

The results of the natural vibration of four different laminations of four-layer angle-ply square plates are discussed next. Table 4 contains the nondimensionalized frequencies of the following four cases of laminates:

Table 1. Nondimensionalized fundamental frequency, $\lambda = \frac{\omega a^2}{h} \sqrt{\rho/E_2}$, of three-layer cross-ply (0°/90°/0°), simply supported plates ($h_1 = h_3 = h/4$, $h_2 = h/2$).

| | | Material I | | | Material II | | |
|---|---|---|---|---|---|---|---|
| | | Finite Element Method | | percentage | Finite Element Method | | percentage |
| b/a | a/h | Plate Theory | 3-D Theory | error | Plate Theory | 3-D Theory | error |
| | 5 | 8.831 | 8.317 | -6.18 | 9.896 | 9.119 | -8.52 |
| 1 | 10 | 12.380<br>(12.233)† | 11.805 | -4.87 | 14.451<br>(14.295)† | 13.370 | -8.09 |
| | 100 | 15.474 | 15.473 | -0.0065 | 19.177 | 18.959 | -1.15 |
| 3 | 10 | - | - | - | 12.555 | 11.338 | -10.734 |

†obtained using 2x2 mesh of nine-node elements.

Table 2. Nondimensionalized frequencies of a square sandwich plate with simply supported boundary conditions. (b/a = 1; $h_1 = h_3 = 0.1h$, $h_2 = 0.8h$; 3D-Theory

| Mode<br>a/h | 1 | 2 | 3 | 4 | 5 | 6 | 7 |
|---|---|---|---|---|---|---|---|
| 10 | 11.132 | 32.881 | 37.153 | 71.787 | 78.006 | 79.616 | 83.380 |

Table 3. Nondimensionalized fundamental frequencies of two-layer (0°/90° or -45°/45°) square plates with simply supported boundary conditions (a/b = 1, a/h = 10, $h_i$ = h/2; 3D-Theory)

| Lamination Scheme | Material I 1 | 2 | 3 | 4 | Material II 1 | 2 | 3 | 4 |
|---|---|---|---|---|---|---|---|---|
| 0°/90° | 9.176 | 44.094 | 44.044 | 60.886 | 10.563 | 48.806 | 48.806 | 67.032 |
| 45°/-45° | 16.668 | 33.816 | 36.723 | 46.929 | 17.826 | 37.690 | 39.260 | 51.305 |

Table 4. Nondimensionalized fundamental frequencies of angle-ply square plates (material I, a/h = 10)

| Mode | -45°/45°/-45° 3D | -45°/45°/-45° Plate | 3D Theory 45°/0°/45° | 3D Theory -30°/30°/-30° | 3D Theory -30°/0°/-30° |
|---|---|---|---|---|---|
| 1 | 16.483 (16.546)† | 15.282 | 18.246 | 16.602 | 16.141 |
| 2 | 34.044 (36.129) | 34.100 | 36.565 | 34.513 | 33.615 |
| 3 | 35.051 (46.273) | 45.062 | 46.484 | 45.975 | 48.984 |
| 4 | 45.753 (64.354) | 46.591 | 49.281 | 47.845 | 52.255 |

†the numbers in parenthesis correspond to the case in which the inplane inertias are omitted.

1. $(-45^0/45^0/-45^0)$, $h_1 = h_3 = h/4$, $h_2 = h/2$, $a/h = 10$
2. $(-45^0/0^0/-45^0)$, $h_1 = h_3 = h/4$, $h_2 = h/2$, $a/h = 10$
3. $(-30^0/30^0/-30^0)$, $h_1 = h_3 = h/4$, $h_2 = h/2$, $a/h = 10$
4. $(-30^0/0^0/-30^0)$, $h_1 = h_3 = h/4$, $h_2 = h/2$, $a/h = 10$

The material properties used are those of material I. Table 4 also contains natural frequencies for Case 1 when the inplane inertias are omitted. It is clear that the effect of the inplane inertia is to reduce the frequencies, and this reduction has a significant effect on higher modes.

Acknowledgement The support of this work by NASA-Lewis Research Center is gratefully acknowledged. The first author is thankful to Dr. C. C. Chamis for the encouragement and support.

## REFERENCES

1. Reissner, E., "The effect of transverse shear deformation on the bending of elastic plate," J. Applied Mechanics, Vol. 12, Trans. of ASME, Vol. 67, A69-A77, 1945.

2. Mindlin, R. D., "Influence of rotatory inertia and shear on flexural motions of isotropic, elastic plates," J. Applied Mechanics, Vol. 18, Trans. ASME, Vol. 73, pp. 31-38, 1951.

3. Reissner, E., and Stavsky, Y., "Bending and stretching of certain types of heterogeneous aerolotropic elastic plates," J. Appl. Mech., Vol. 28, 1961, pp. 402-408.

4. Yang, P. C., Norris, C. H., and Stavsky, Y., "Elastic wave propagation in heterogeneous plates," Int. J. Sol. Struct., Vol. 2, 1966, pp. 665-684.

5. Whitney, J. M., and Pagano, N. J., "Shear deformation in heterogeneous anisotropic plates," J. Appl. Mech., Vol. 37, 1970, pp. 1031-1036.

6. Reddy, J. N., and Chao, W. C., "A comparison of closed-form and finite element solutions of thick laminated anisotropic rectangular plates," Nuclear Engineering and Design, Vol. 64, 1981, 153-167.

7. Reddy, J. N., "A penalty plate-bending element for the analysis of laminated anisotropic plates," Int. J. Num. Meth. Engng., Vol. 15, 1980, pp. 1187-1206.

8. Reddy, J. N. and Chao, W. C., "Non-linear bending of thick rectangular, laminated composite plates," Int. J. Non-Linear Mechanics, Vol. 16, 1981, pp. 291-301.

9. Reddy, J. N. and Chao, W. C., "Large deflection and large amplitude free vibrations of laminated composite-material plates," Computers and Structures, Vol. 13, No. 2, pp. 341-347, 1981.

10. Reddy, J. N., "On the solutions to forced motions of rectangular composite plates," J. Applied Mechanics, Vol. 49, pp. 403-408, 1982.

11. Reddy, J. N. and Chao, W. C., "Nonlinear oscillations of laminated, anisotropic, rectangular plates," J. Applied Mechanics, Vol. 49, pp. 396-402, 1982.

12. Reddy, J. N., "Geometrically nonlinear transient analysis of laminated composite plates," AIAA Journal, to appear.

13. Dana, J. R., and Barker, R. M., "Three dimensional analysis for the stress distribution near circular holes in laminated composites," Research report No. VPI-E-74-18, Virginia Polytechnic Institute and State University, August 1974.

14. Putcha, N. S. and Reddy, J. N., "Three-dimensional finite-element analysis of layered composite plates," Advances in Aerospace Structures, Winter Annual Meeting of ASME, Nov. 14-19, 1982, Phoenix, Arizona.

15. Kuppusamy, T. and Reddy, J. N., "Nonlinear analysis of cross-ply rectangular plates by a 3-D element," Report VPI-E-82-31, Virginia Polytechnic Institute and State University, Blacksburg, VA, 1982.

# A THREE-DIMENSIONAL NONLINEAR ANALYSIS OF CROSS-PLY RECTANGULAR COMPOSITE PLATES

T. Kuppusamy[1] and J. N. Reddy[2]
Virginia Polytechnic Institute and State University
Blacksburg, VA 24061

Abstract

The results of a three-dimensional, geometrically nonlinear, finite-element analysis of the bending of cross-ply laminated anisotropic composite plates are presented. Individual laminae are assumed to be homogeneous, orthotropic and linearly elastic. A fully three-dimensional isoparametric finite element with eight nodes (i.e., linear element) and 24 degrees of freedom (three displacement components per node) is used to model the laminated plate. The finite element results of the linear analysis are found to agree very well with the exact solutions of cross-ply laminated rectangular plates under sinusoidal loading. The finite element results of the three-dimensional, geometrically nonlinear analysis are compared with those obtained by using a shear deformable, geometrically nonlinear, plate theory. It is found that the deflections predicted by the shear deformable plate theory are in fair agreement with those predicted by 3-D elasticity theory.

[1]Assistant Professor of Civil Engineering.

[2]Professor of Engineering Science and Mechanics.

# 1. INTRODUCTION

Composite materials exhibit higher stiffness-to-weight ratios and increased corrosion resistance compared to isotropic materials. The anisotropic material properties of layered composites can be varied by varying the fiber orientation and stacking sequence. While this feature gives the designer an added degree of flexibility, the stiffness mismatch of the orthotropic layers bonded together with different fiber orientations leads to interlaminar stresses in the vicinity of free edges. For certain stacking sequences, loading, and boundary conditions interlaminar stresses can be so large that they dictate the design of the structure.

Analyses of layered composite plates can be divided into two groups: (i) analyses based on a laminate plate theory, and (ii) analyses based on a three-dimensional laminated (elasticity) theory. The laminated plate theory is the extension of the classical plate theory (CPT) or the Reissner-Mindlin shear-deformable plate theory (SDT) to layered composite plates. The first lamination theory including bending-stretching coupling is apparently due to Reissner and Stavsky [1]. Yang, Norris, and Stavsky [2] presented a generalization of the Reissner-Mindlin thick-plate theory for homogeneous, isotropic plates to arbitrarily laminated anisotropic plates. Whitney and Pagano [3] (also see Reddy and Chao [4]) presented closed-form solutions to the theory when applied to certain cross-ply and angle-ply rectangular plates. Reddy [5] presented a finite-element analysis of the lamination theory. A higher-order lamination theory that accounts for a cubic variation (as opposed to linear in [2-5]) of the inplane displacements and quadratic variation of the transverse displacement through the

thickness was presented by Lo, Christensen, and Wu [6], and hybrid-stress finite-element analysis of the theory was presented by Spilker [7].

In laminated plate theory it is assumed that the laminate is in a state of plane stress (as assumption carried from the classical plate theory) and integrals through the thickness of a laminate are equal to the sum of integrals through the thickness of individual laminae. These assumptions lead to inaccurate prediction of interlaminar stresses at the free edges, although the solution is reasonably accurate away from free edges. The laminate plate theory is not accurate in a boundary layer region which extends inward from the edge to a distance approximately equal to the laminate thickness.

The fully three-dimensional laminate theory is an extension of the elasticity theory of a three-dimensional solid composed of layers of different material properties. Pipes and Pagano [8] and Pipes [9] used a finite-difference technique to solve the quasi-three-dimensional, linear, elasticity equations for laminates (also see Hsu and Herakovich [10]). Lin [11], Dana [12], and Dana and Barker [13] used a cubic, three-dimensional, isoparametric element with 72 degrees of freedom to analyze laminated plates (also see Putcha and Reddy [14]). The numerical results in these studies agree very well with those of Pagano [15,16].

The present study is motivated by the lack of finite-element results for three-dimensional, geometrically nonlinear analysis of layered anisotropic composite plates. A finite-element formulation of the geometrically nonlinear theory of a laminated, three-dimensional, elastic continuum is presented. Numerical results of the linear as well

as nonlinear analysis are presented for several cross-ply plate problems. The formulation is validated by comparing the present results of the linear analysis with those of Pagano [15,16]. The results of the nonlinear analysis should serve as bench mark results for future investigations.

## 2. GOVERNING EQUATIONS

Consider a laminate ($\Omega$) composed of N orthotropic layers with axes of elastic symmetry parallel to the plate axes. The laminate is subjected to normal traction $\hat{t}_3 = q(x_1, x_2)$ at its upper surface (i.e., $x_3 = h/2$). The constitutive equations for any layer are given by

$$\begin{Bmatrix} \bar{\sigma}_{11} \\ \bar{\sigma}_{2} \\ \bar{\sigma}_{33} \\ \bar{\sigma}_{23} \\ \bar{\sigma}_{13} \\ \bar{\sigma}_{12} \end{Bmatrix} = \begin{bmatrix} \bar{C}_{11} & \bar{C}_{12} & \bar{C}_{13} & 0 & 0 & 0 \\ \bar{C}_{12} & \bar{C}_{22} & \bar{C}_{23} & 0 & 0 & 0 \\ \bar{C}_{13} & \bar{C}_{23} & \bar{C}_{33} & 0 & 0 & 0 \\ 0 & 0 & 0 & \bar{C}_{44} & 0 & 0 \\ 0 & 0 & 0 & 0 & \bar{C}_{55} & 0 \\ 0 & 0 & 0 & 0 & 0 & \bar{C}_{66} \end{bmatrix} \begin{Bmatrix} \bar{\varepsilon}_{11} \\ \bar{\varepsilon}_{22} \\ \bar{\varepsilon}_{33} \\ 2\bar{\varepsilon}_{23} \\ 2\bar{\varepsilon}_{13} \\ 2\bar{\varepsilon}_{12} \end{Bmatrix} . \tag{1}$$

where $\bar{\sigma}_{ij}$ and $\bar{\varepsilon}_{ij}$ are the components of the stress and strain tensors, respectively, defined in the material-coordinates, and $\bar{C}_{ij}$ are the material stiffness coefficients. The coefficients, $\bar{C}_{ij} = \bar{C}_{ji}$, are given in terms of the engineering constants by (see Jones [17])

$$\bar{C}_{11} = E_1(1 - \nu_{23}\nu_{32})/\Delta$$

$$\bar{C}_{12} = E_2(\nu_{12} + \nu_{32}\nu_{13})\Delta$$

$$\bar{C}_{13} = E_3(\nu_{13} + \nu_{12}\nu_{23})/\Delta$$

$$\bar{C}_{22} = E_2(1 - \nu_{13}\nu_{31})/\Delta$$

$$\bar{C}_{23} = E_3(\nu_{23} + \nu_{21}\nu_{13})/\Delta$$

$$\bar{C}_{33} = E_3(1 - \nu_{12}\nu_{21})/\Delta$$

$$\bar{C}_{44} = G_{23} \quad , \quad \bar{C}_{55} = G_{13} \quad , \quad \bar{C}_{66} = G_{12}$$

$$\Delta = (1 - \nu_{12}\nu_{21} - \nu_{23}\nu_{32} - \nu_{31}\nu_{13} - 2\nu_{21}\nu_{31}\nu_{32}), \tag{2}$$

where

$E_1, E_2, E_3$ = Young's moduli in 1, 2 and 3 (material) directions, respectively

$\nu_{ij}$ = Poisson's ratio for transverse strain in the J-direction when stressed in the i-direction

$G_{23}, G_{13}, G_{12}$ = Shear moduli in the 2-3, 1-3, and 1-2 planes, respectively. (3)

In view of the reciprocal relations

$$\frac{\nu_{ij}}{E_i} = \frac{\nu_{ji}}{E_j}, \tag{4}$$

there are only nine independent elastic constants for an orthotropic elastic medium.

The constitutive equations (1) when transformed to the plate coordinate system take the form

$$\begin{Bmatrix} \sigma_{11} \\ \sigma_{22} \\ \sigma_{33} \\ \sigma_{23} \\ \sigma_{13} \\ \sigma_{12} \end{Bmatrix} = \begin{bmatrix} C_{11} & C_{12} & C_{13} & 0 & 0 & 0 \\ C_{12} & C_{22} & C_{23} & 0 & 0 & 0 \\ C_{13} & C_{23} & C_{33} & 0 & 0 & 0 \\ 0 & 0 & 0 & C_{44} & 0 & 0 \\ 0 & 0 & 0 & 0 & C_{55} & 0 \\ 0 & 0 & 0 & 0 & 0 & C_{66} \end{bmatrix} \begin{Bmatrix} \varepsilon_{11} \\ \varepsilon_{22} \\ \varepsilon_{33} \\ \gamma_{23} \\ \gamma_{13} \\ \gamma_{22} \end{Bmatrix} \tag{5}$$

where $C_{ij}$ are the transformed plate stiffnesses.

The nonlinear kinematic description of an elastic body yields the following equations of equilibrium (in the absence of body forces and moments)

$$\frac{\partial}{\partial x_j}\left[\sigma_{ij}\left(\delta_{mi} + \frac{\partial u_m}{\partial x_i}\right)\right] = 0 \quad , \quad (i,j = 1,2,3), \tag{6}$$

wherein $\delta_{mi}$ denotes the Kronecker delta symbol, and the summation convention on repeated subscripts is used. The strain-displacement equations of the large-deflection theory of elasticity are given by

$$\varepsilon_{ij} = \frac{1}{2}\left(\frac{\partial u_i}{\partial x_j} + \frac{\partial u_j}{\partial x_i} + \frac{\partial u_m}{\partial x_i}\frac{\partial u_m}{\partial x_j}\right). \tag{7}$$

To complete the description of the field equations, Eqs. (4)-(6), and (7) should be adjoined by boundary conditions. At any point of the boundary of the body one should specify one of the following two types of boundary conditions:

(i) essential (or geometric) boundary conditions

$$u_m = \hat{u}_m$$

(ii) natural (or dynamic) boundary conditions

$$t_m \equiv n_j \sigma_{ij}(\delta_{mi} + u_{m,i}) = \hat{t}_m. \tag{8}$$

Here $n_j$ denotes the j-th component of the unit normal to the boundary, $t_m$ the m-th component of the boundary traction, and $\hat{u}_m$ and $\hat{t}_m$ denote specified values.

## 3. FINITE-ELEMENT FORMULATION

Here we present a displacement finite-element model of the equations (3)-(8). To this end we construct the variational formulation of the equations over an arbitrary element $\Omega^{(e)}$ of the finite-element mesh. We have (see [18, p. 382])

$$0 = \int_{\Omega^{(e)}} \{\delta u_{m,j}\sigma_{ij}(\delta_{mi} + u_{m,i})\}dx_1dx_2dx_3 - \int_{\Gamma^{(e)}} t_m\delta u_m ds \qquad (9)$$

Here $\delta$ denotes the variational symbol, and $\sigma_{ij}$ is given in terms of $u_i$ via Eqs. (4) and (7).

The displacements $u_m$ are interpolated by expressions of the form,

$$u_m = \sum_{\alpha=1}^{8} u_m^\alpha \phi_\alpha \quad (m = 1,2,3) \qquad (10)$$

where $\phi_\alpha(x,y,z)$ $(\alpha = 1,2,\ldots,8)$ are the trilinear interpolation functions of the eight-node isoparametric element in three dimensions, and $u_m^\alpha$ denotes the value of $u_m$ at node $\alpha$. Substituting Eq. (10) into (9), we obtain

$$\sum_{n=1}^{3} \sum_{\beta=1}^{8} K_{\alpha\beta}^{mn} u_n^\beta + F_\alpha^m = 0 \quad , \quad (m = 1,2,3;\ \alpha = 1,2,\ldots,8), \qquad (11)$$

where

$$K_{\alpha\beta}^{mn} = \int_{\Omega^{(e)}} \frac{\partial\phi_\alpha}{\partial x_j} [\sigma_{nj}(\delta_{mn} + \sum_{\beta=1}^{8} u_m^\beta \frac{\partial\phi_\beta}{\partial x_n})]dx_1dx_2dx_3$$

$$F_\alpha^m = \int_{\Gamma^{(e)}} t_m\phi_\alpha ds \quad , \quad (j,m,n = 1,2,3) \qquad (12)$$

Every isoparametric finite element $\Omega^{(e)}$ of the finite-element mesh can be generated from the master element via the transformation (see Figure 2)

$$x_i = x_i(\xi_1,\xi_2,\xi_3)$$

$$= \sum_{\alpha=1}^{8} x_i^{\alpha} \phi_{\alpha}(\xi_1, \xi_2, \xi_3) \quad (i = 1,2,3) \tag{13}$$

where $x_i^{\alpha}$ are the global coordinates of the element nodes and $\xi_i (i = 1,2,3)$ are the local coordinates. Therefore, the integrals in Eq. (12) can be transformed to the master element and evaluated numerically using the Gauss quadrature. The transformation of $\frac{\partial \phi_\alpha}{\partial x_i}$ to $\frac{\partial \phi_\alpha}{\partial \xi_1}$ is performed as follows:

$$\underset{3\times 1}{\left\{\frac{\partial \phi_\alpha}{\partial x_i}\right\}} = [J]^{-1} \underset{3\times 1}{\left\{\frac{\partial \phi_\alpha}{\partial \xi_i}\right\}}$$

$$dx_1 dx_2 dx_3 = (\det [J]) d\xi_1 d\xi_2 d\xi_3$$

where

$$\underset{3\times 3}{[J]} = \underset{3\times 8}{\begin{bmatrix} \frac{\partial \phi_1}{\partial \xi_1} & \frac{\partial \phi_2}{\partial \xi_1} & \cdots & \frac{\partial \phi_8}{\partial \xi_1} \\ \frac{\partial \phi_1}{\partial \xi_2} & \frac{\partial \phi_2}{\partial \xi_2} & \cdots & \frac{\partial \phi_8}{\partial \xi_2} \\ \frac{\partial \phi_1}{\partial \xi_3} & \frac{\partial \phi_2}{\partial \xi_3} & \cdots & \frac{\partial \phi_8}{\partial \xi_3} \end{bmatrix}} \underset{8\times 3}{\begin{bmatrix} x_1^1 & x_2^1 & x_3^1 \\ x_1^2 & x_2^2 & x_3^2 \\ \vdots & \vdots & \vdots \\ x_1^8 & x_2^8 & x_3^8 \end{bmatrix}} \tag{14}$$

For example, consider

$$\int_{\Omega^{(e)}} \frac{\partial \phi_\alpha}{\partial x_i} \frac{\partial \phi_\beta}{\partial x_j} dx_1 dx_2 dx_3 = \int_{-1}^{1} \int_{-1}^{1} \int_{-1}^{1} F_{\alpha\beta}^{ij} (\xi_1, \xi_2, \xi_3) d\xi_1 d\xi_2 d\xi_3$$

$$= \sum_{I=1}^{m} \sum_{J=1}^{m} \sum_{K=1}^{m} F_{\alpha\beta}^{ij} (P_I, P_J, P_K) W_I W_J W_K \tag{15}$$

where $P_I$ and $W_I$ are the Gauss points and weights, respectively, and the integrand $F_{\alpha\beta}^{ij}$ $(i,j = 1,2,3;\ \alpha,\beta = 1,2,\ldots,8)$ is given by

$$F_{\alpha\beta}^{ij} = \left(\sum_{k=1}^{3} J_{ik}^{*} \frac{\partial\psi_\alpha}{\partial\xi_k}\right) \left(\sum_{\ell=1}^{3} J_{j\ell}^{*} \frac{\partial\psi_\beta}{\partial\xi_\ell}\right) \det\,[J] \qquad (16)$$

$K_{k\ell}^{*}$ being the elements of the inverse of the Jacobian matrix, [J]. This procedure can be implemented on a digital computer, and the element coefficient matrices in Eq. (10) can be evaluated numerically. It is well known that when the ratio of side to thickness of the plate is very large (i.e., when the plate is thin, say a/h > 20) one should use reduced integration to evaluate the shear terms (i.e., terms involving $C_{44}$, $C_{45}$, and $C_{55}$). For a trilinear element, 1x1x1 Gauss quadrature must be used to evaluate the coefficients of $Q_{44}$, $Q_{55}$, and 2x2x2 Gauss rule to evaluate all other terms.

Since the coefficient matrix [K] depends on the unknown solution vector {u}, one should employ an iterative solution procedure to solve the finite-element equations. Here we use the Picard type iterative technique, which begins with an assumed displacement field (usually, set to zero to obtain the linear solution) to compute [K] at the beginning of the first iteration. In subsequent iterations, solution obtained from the previous iterations is used to compute [K]. The iteration is continued until the solutions obtained in two consecutive iterations differ by a preassigned error margin (say, $10^{-4}$). It is more economical to use load incremental methods in conjunction with the iterative technique described above. In other words, for each increment of the load the increment to the nonlinear solution is obtained (see [19]).

## 4. DISCUSSION OF THE NUMERICAL RESULTS

### Results of the Linear Analysis

In order to validate the present formulation and element, first the linear analysis of a symmetric three-layer square laminate with the $\bar{x}_1$-direction (of material principal axes) coinciding with the $x_1$-direction (of the plate axes) in the outer layers and the $\bar{x}_2$-direction parallel to the $x_1$-axis in the center layer is performed. The thickness of the outer layers is assumed to be one-half of the thickness of the center layer ($h_1 = h_3 = h/4$, $h_2 = h/2$). The loading is assumed to be sinusoidal with respect to the $x_1$-$x_2$ plane,

$$\hat{t}_3 \equiv q(x_1, x_2) = q_0 \cos\frac{\pi x_1}{a} \cos\frac{\pi x_2}{b} \tag{17}$$

and the boundary conditions are of the simply supported type which allow normal displacement on the boundary, but prevent tangential displacement. For a quarter plate these imply

$$\begin{aligned}
&\text{at } x_1 = a/2: \quad \hat{u}_2 = \hat{u}_3 = \hat{t}_x = 0 \\
&\text{at } x_1 = 0: \quad \hat{u}_1 = 0,\ \hat{t}_y = 0,\ \hat{t}_z = 0 \\
&\text{at } x_2 = b/2: \quad \hat{u}_1 = u_3 = \hat{t}_y = 0 \\
&\text{at } x_2 = 0: \quad \hat{u}_2 = 0,\ \hat{t}_x = 0,\ \hat{t}_z = 0.
\end{aligned} \tag{18}$$

The material of the laminae is assumed to have the following values for the engineering constants

$$E_1 = 1.724 \times 10^8 \text{ kN/m}^2 \ (25 \times 10^6 \text{ psi})$$

$$E_2 = E_3 = 6.89 \times 10^6 \text{ kN/m}^2 \ (10^6 \text{ psi})$$

$$G_{12} = G_{13} = 3.45 \times 10^6 \text{ kN/m}^2 \ (0.5 \times 10^6 \text{ psi}) \tag{19}$$

$$G_{23} = 13.78 \times 10^6 \text{ kN/m}^2 \ (0.2 \times 10^6 \text{ psi})$$

$$\nu_{12} = \nu_{31} = \nu_{32} = 0.25$$

The following nondimensionalization is used to present the displacements and stresses:

$$\bar{u}_1 = \frac{E_2 h^2}{q_o a^3} u_1 \quad , \quad \bar{u}_3 = \frac{(E_2 h^3 u_3) 10^2}{q_o a^4}$$

$$(\bar{\sigma}_1, \bar{\sigma}_2, \bar{\sigma}_{12}) = \frac{h^2}{q_o a^2} (\sigma_1, \sigma_2, \sigma_{12}) \quad , \quad (\bar{\sigma}_{23}, \bar{\sigma}_{13}) = \frac{h}{q_o a} (\sigma_{23}, \sigma_{13}) \tag{20}$$

The nondimensionalized center deflection $\bar{u}_3(0,0,0)$ obtained using the laminated plate theory [4,5] and the elasticity theory are presented in Table 1. One can conclude from the results that the finite element results obtained by using the reduced integration (R) are in good agreement with the analytical solution of Pagano [16], and the shear-deformable plate theory solution [4,5] differs from the 3-D elasticity solution by about 10% for the problem at hand. The classical plate theory (CPT) solution differs from the shear deformable plate theory (SDPT) by 35% for side to thickness ratio of $a/h = 10$.

The nondimensionalized stresses ($\bar{\sigma}_1$, $\bar{\sigma}_5 = \bar{\sigma}_{13}$, $\bar{\sigma}_6 = \bar{\sigma}_{12}$) for the problem are compared in Table 2. We observe that for $a/h > 50$ the results obtained using the reduced integration are in good agreement with the analytical solutions, and for $a/h < 20$ the full integration gives better results.

Nondimensionalized center deflection and stresses of three-layer ($h_i = h/3$) rectangular plates ($b/a = 3$) of cross-ply (0°/90°/0°)

Table 1 Nondimensionalized center deflection† in a square cross-ply (0°/90°/0°) plate ($h_1 = h_3 = h/4$, $h_2 = h/2$) under sinusoidal loading ($E_2 = E_3$, $E_1 = 25E_2$, $G_{12} = G_{13} = 0.5E_2$, $G_{23} = 0.2E_2$, $\nu_{12} = \nu_{23} = \nu_{13} = 0.25$)

| | | Elasticity Solution | | | | Shear Deformable Plate Solution[4] | | | | | |
|---|---|---|---|---|---|---|---|---|---|---|---|
| a/h | Pagano [16] | 2x2x3 F | 4x4x3 F | 2x2x3 R | 4x4x3 R | CFS | 2x2 F | 4x4 F | 2x2 R | 4x4 R | CPT |
| 2 | 5.075 | 5.052 | 4.986 | 5.341 | 5.051 | 5.063 | 5.253 | 5.109 | 5.525 | 5.170 | 0.431 |
| 4 | 1.937 | 1.841 | 1.872 | 1.983 | 1.906 | 1.709 | 1.722 | 1.713 | 1.814 | 1.734 | 0.431 |
| 10 | 0.737 | 0.614 | 0.694 | 0.734 | 0.728 | 0.663 | 0.590 | 0.643 | 0.665 | 0.663 | 0.431 |
| 20 | 0.513 | 0.307 | 0.437 | 0.496 | 0.506 | 0.491 | 0.324 | 0.435 | 0.476 | 0.487 | 0.431 |
| 50 | 0.445 | 0.091 | 0.124 | 0.423 | 0.438 | 0.441 | 0.105 | 0.245 | 0.420 | 0.436 | 0.431 |
| 100 | 0.435 | 0.027 | 0.089 | 0.412 | 0.429 | 0.434 | 0.032 | 0.103 | 0.412 | 0.428 | 0.431 |

† $\bar{u}_3(0,0,\frac{h}{2})$; mesh shown is for a quarter plate; boundary conditions are the same as those shown in Eq. (18).

Table 2. Comparison of nondimensional stresses† for three-layer (0°/90°/0°) cross-ply square plate under sinusoidal loading ($a/b = 1$, $h_1 = h_3 = h/4$, $h_2 = h/2$).

| | | 3D-Elasticity Theory | | | | | Plate Theory [4] | | | |
|---|---|---|---|---|---|---|---|---|---|---|
| $\frac{a}{h}$ | Stress type | Pagano [16] | 2x2x3 F | 4x4x3 F | 2x2x3 R | 4x4x3 R | 2x2 F | 4x4 F | 2x2 R | 4x4 R |
| | $\bar{\sigma}_1$ | 1.388 | 0.603 | 0.676 | 0.133 | 0.165 | 0.259 | 0.318 | 0.259 | 0.318 |
| 2 | $\bar{\sigma}_5$ | 0.153 | 0.224 | 0.224 | 0.179 | 0.197 | 0.242 | 0.286 | 0.255 | 0.289 |
| | $\bar{\sigma}_6$ | 0.086 | 0.047 | 0.053 | 0.025 | 0.031 | 0.027 | 0.033 | 0.028 | 0.033 |
| | $\bar{\sigma}_1$ | 0.720 | 0.389 | 0.456 | 0.185 | 0.232 | 0.302 | 0.377 | 0.306 | 0.379 |
| 4 | $\bar{\sigma}_5$ | 0.219 | 0.182 | 0.209 | 0.138 | 0.205 | 0.276 | 0.330 | 0.293 | 0.335 |
| | $\bar{\sigma}_6$ | 0.047 | 0.029 | 0.034 | 0.021 | 0.025 | 0.023 | 0.029 | 0.024 | 0.029 |
| | $\bar{\sigma}_1$ | 0.599 | 0.326 | 0.425 | 0.268 | 0.331 | 0.334 | 0.451 | 0.380 | 0.467 |
| 10 | $\bar{\sigma}_5$ | 0.301 | 0.235 | 0.281 | 0.147 | 0.286 | 0.316 | 0.389 | 0.353 | 0.400 |
| | $\bar{\sigma}_6$ | 0.028 | 0.028 | 0.022 | 0.015 | 0.018 | 0.016 | 0.022 | 0.019 | 0.023 |
| | $\bar{\sigma}_1$ | 0.543 | 0.240 | 0.391 | 0.298 | 0.364 | 0.265 | 0.437 | 0.404 | 0.494 |
| 20 | $\bar{\sigma}_5$ | 0.328 | 0.421 | 0.342 | 0.277 | 0.312 | 0.303 | 0.395 | 0.373 | 0.420 |
| | $\bar{\sigma}_6$ | 0.023 | 0.010 | 0.017 | 0.013 | 0.016 | 0.011 | 0.018 | 0.017 | 0.021 |
| | $\bar{\sigma}_1$ | 0.539 | 0.083 | 0.234 | 0.308 | 0.376 | 0.098 | 0.279 | 0.413 | 0.504 |
| 50 | $\bar{\sigma}_5$ | 0.337 | 0.755 | 0.990 | 0.286 | 0.321 | 0.252 | 0.348 | 0.380 | 0.427 |
| | $\bar{\sigma}_6$ | 0.021 | 0.003 | 0.009 | 0.012 | 0.015 | 0.004 | 0.011 | 0.016 | 0.020 |
| | $\bar{\sigma}_1$ | 0.271 | 0.025 | 0.095 | 0.310 | 0.378 | 0.030 | 0.120 | 0.414 | 0.505 |
| 100 | $\bar{\sigma}_5$ | 0.339 | 0.877 | 1.569 | 0.287 | 0.274 | 0.230 | 0.298 | 0.381 | 0.428 |
| | $\bar{\sigma}_6$ | 0.339 | 0.001 | 0.004 | 0.012 | 0.015 | 0.001 | 0.005 | 0.016 | 0.020 |

†The stresses in the finite-element analysis are computed at the Gauss points.

Table 3. Nondimensionalized center deflection in a rectangular (b = 3a) cross-ply (0°/90°/0°) plate ($h_1 = h_2 = h_3 = h/3$) under sinusoidal loading (BC1, $E_2 = E_3$, $E_1 = 25E_2$, $G_{12} = G_{13} = 0.5E_2$, $G_{23} = 0.2E_2$, $\nu_{12} = \nu_{23} = 0.25$)

| a/h | Pagano [15] | Elasticity Solution 2x2x3 | 4x4x3 | 2x2x3 | 4x4x3 | Shear Deformable Plate Solution [5] CFS | 2x2 | 4x4 | 2x2 | 4x4 | CPT Solution |
|---|---|---|---|---|---|---|---|---|---|---|---|
| 2 | 8.17 | 7.953 | 7.831 | 8.410 | 7.934 | 10.11 | 8.153 | 7.900 | 8.600 | 8.000 | 0.480 |
| 4 | 2.82 | 2.702 | 2.716 | 2.905 | 2.764 | 2.97 | 2.418 | 2.376 | 2.655 | 2.405 | 0.480 |
| 10 | 0.919 | 0.801 | 0.872 | 0.915 | 0.902 | 0.93 | 0.748 | 0.788 | 0.810 | 0.804 | 0.480 |
| 20 | 0.610 | 0.411 | 0.540 | 0.589 | 0.600 | 0.60 | 0.425 | 0.530 | 0.560 | 0.574 | 0.480 |
| 50 | 0.508 | 0.137 | 0.305 | 0.494 | 0.513 | 0.51 | 0.150 | 0.327 | 0.490 | 0.509 | 0.480 |
| 100 | 0.503 | 0.042 | 0.134 | 0.481 | 0.501 | 0.50 | 0.050 | 0.153 | 0.480 | 0.500 | 0.480 |

Table 4. Comparison of nondimensionalized stresses† for three-layer cross-ply (0°/90°/0°) square plate under sinusoidal loading ($a/b = 1$, $h_1 = h/3$)

| $\frac{a}{h}$ | Stress Type | Pagano [15] | 3D-Elasticity Theory 2x2x3 F | 4x4x3 F | 2x2x3 R | 4x4x3 R | Plate Theory [5] 2x2 F | 4x4 F | 2x2 R | 4x4 R |
|---|---|---|---|---|---|---|---|---|---|---|
| | $\bar{\sigma}_1$ | 0.938 | 0.550 | 0.619 | 0.097 | 0.122 | 0.274 | 0.337 | 0.273 | 0.336 |
| 2 | $\bar{\sigma}_5$ | 0.309 | 0.257 | 0.267 | 0.212 | 0.236 | 0.124 | 0.295 | 0.263 | 0.290 |
| | $\bar{\sigma}_6$ | 0.070 | 0.044 | 0.050 | 0.025 | 0.032 | 0.037 | 0.046 | 0.038 | 0.046 |
| | $\bar{\sigma}_1$ | 0.755 | 0.400 | 0.470 | 0.162 | 0.205 | 0.324 | 0.406 | 0.330 | 0.408 |
| 4 | $\bar{\sigma}_5$ | 0.282 | 0.221 | 0.247 | 0.209 | 0.244 | 0.284 | 0.340 | 0.303 | 0.345 |
| | $\bar{\sigma}_6$ | 0.051 | 0.031 | 0.036 | 0.021 | 0.025 | 0.028 | 0.034 | 0.030 | 0.035 |
| | $\bar{\sigma}_1$ | 0.590 | 0.325 | 0.424 | 0.244 | 0.301 | 0.343 | 0.464 | 0.392 | 0.481 |
| 10 | $\bar{\sigma}_5$ | 0.357 | 0.271 | 0.333 | 0.301 | 0.343 | 0.311 | 0.382 | 0.348 | 0.393 |
| | $\bar{\sigma}_6$ | 0.029 | 0.017 | 0.022 | 0.014 | 0.017 | 0.017 | 0.023 | 0.020 | 0.024 |
| | $\bar{\sigma}_1$ | 0.552 | 0.233 | 0.381 | 0.267 | 0.327 | 0.267 | 0.440 | 0.408 | 0.499 |
| 20 | $\bar{\sigma}_5$ | 0.385 | 0.426 | 0.361 | 0.327 | 0.369 | 0.295 | 0.381 | 0.360 | 0.405 |
| | $\bar{\sigma}_6$ | 0.023 | 0.010 | 0.016 | 0.012 | 0.014 | 0.011 | 0.019 | 0.017 | 0.021 |
| | $\bar{\sigma}_1$ | 0.541 | 0.080 | 0.225 | 0.274 | 0.335 | 0.098 | 0.280 | 0.414 | 0.504 |
| 50 | $\bar{\sigma}_5$ | 0.393 | 0.757 | 0.992 | 0.335 | 0.377 | 0.248 | 0.338 | 0.363 | 0.408 |
| | $\bar{\sigma}_6$ | 0.022 | 0.003 | 0.009 | 0.011 | 0.013 | 0.004 | 0.011 | 0.017 | 0.020 |
| | $\bar{\sigma}_1$ | 0.539 | 0.024 | 0.092 | 0.276 | 0.336 | 0.030 | 0.120 | 0.414 | 0.505 |
| 100 | $\bar{\sigma}_5$ | 0.395 | 0.878 | 1.570 | 0.337 | 0.378 | 0.229 | 0.290 | 0.364 | 0.409 |
| | $\bar{\sigma}_6$ | 0.021 | 0.001 | 0.004 | 0.011 | 0.013 | 0.001 | 0.005 | 0.016 | 0.020 |

†The stresses in the finite-element analysis are computed at the Gauss points.

construction are presented in Tables 3 and 4. The loading, boundary conditions, and material properties are the same as those given in Eqs. (17), (18), and (19), respectively. The finite-element results are in good agreement with the corresponding exact solutions [15] and plate theory solutions [5].

Results of the Nonlinear Analysis

First, geometrically nonlinear analysis of isotropic plates is performed and the results are compared with the results available in the literature. A square isotropic plate ($\nu = 0.3$) subjected to uniformly distributed load is analyzed using simply supported boundary conditions. Due to the biaxial symmetry, only one quadrant of the plate is modeled with 4x4x1 mesh of linear elements. Since membrane and bending contributions dominate the stiffness matrix, full integration is used to evaluate the element matrices. The present results for the center deflection and stresses are compared in Figs. 1 and 2 with the nonlinear thin plate theory (i.e., the von Karman plate theory) solutions available in the literature [20,21]. From the results of the isotropic plate one can conclude that the nonlinearity exhibited by the 3-D elasticity theory is relatively smaller than that included in the classical von Karman plate theory [21] but larger than that in the shear deformable plate theory [20].

Next, a symmetric cross-ply (0°/90°/0°) square plate under uniformly distributed load is analyzed. The boundary conditions and material properties are given by Eqs. (18) and (19), respectively. The 3-D elasticity results for center deflection and stresses are compared with the shear deformable plate theory results [20] in Figs. 3-5. The effect of thickness (i.e., ratio of side to thickness) on the

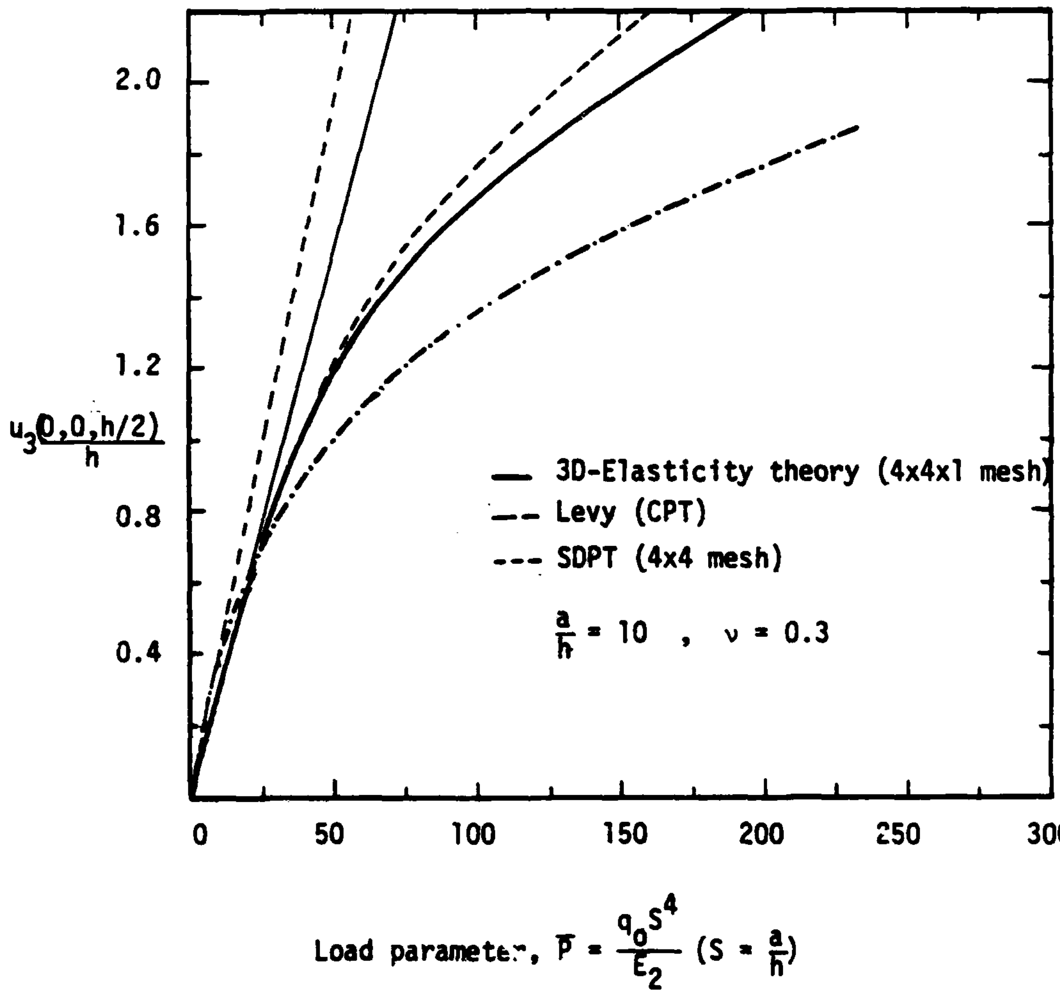


Figure 1 Load-deflection curves for simply supported isotropic ($\nu = 0.3$) square plate under uniform load.

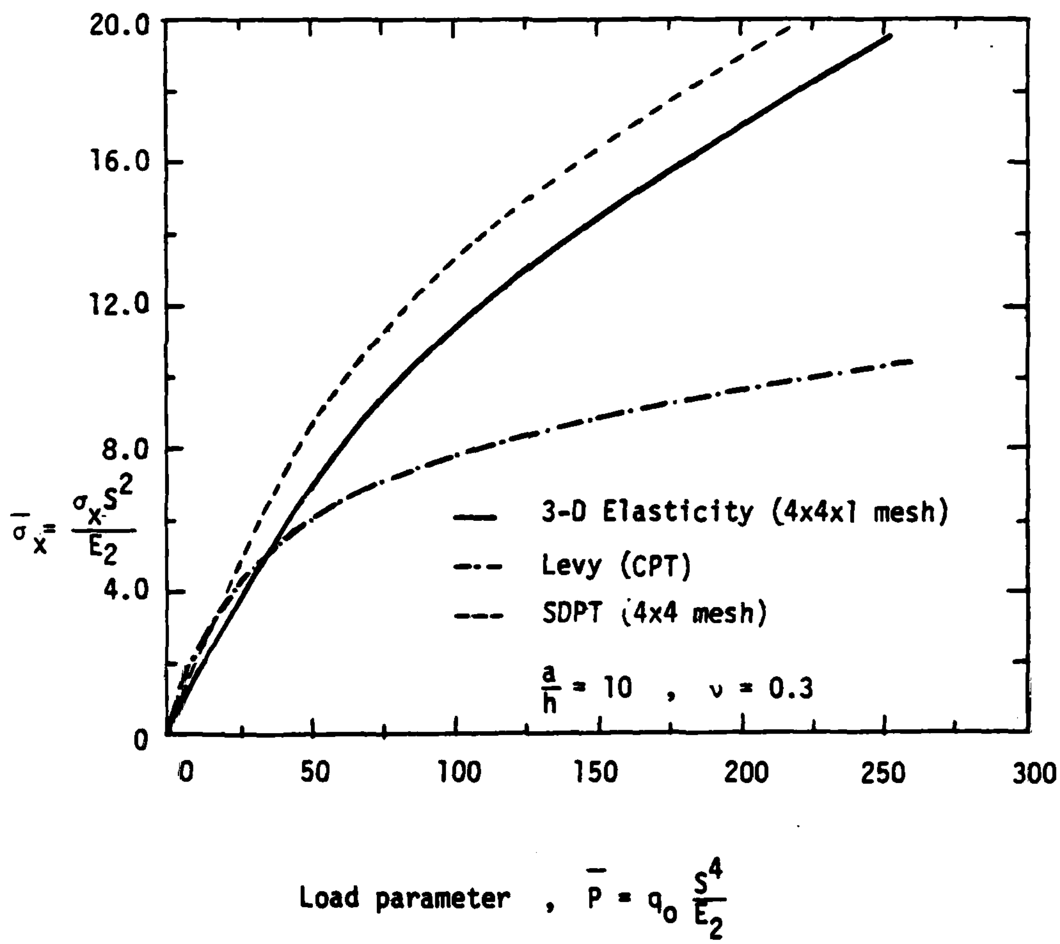


Figure 2 Center normal stress versus the load parameter for simply supported isotropic ($\nu = 0.3$) square plate under uniform load ($\bar{\sigma}_x$ is computed at $\underset{\sim}{x}$ = (0.0264, 0.0264, 0.0789 in 3-D elasticity theory and $\underset{\sim}{x}$ = (0.0625, 0.0625, 0.1) in the plate theory)

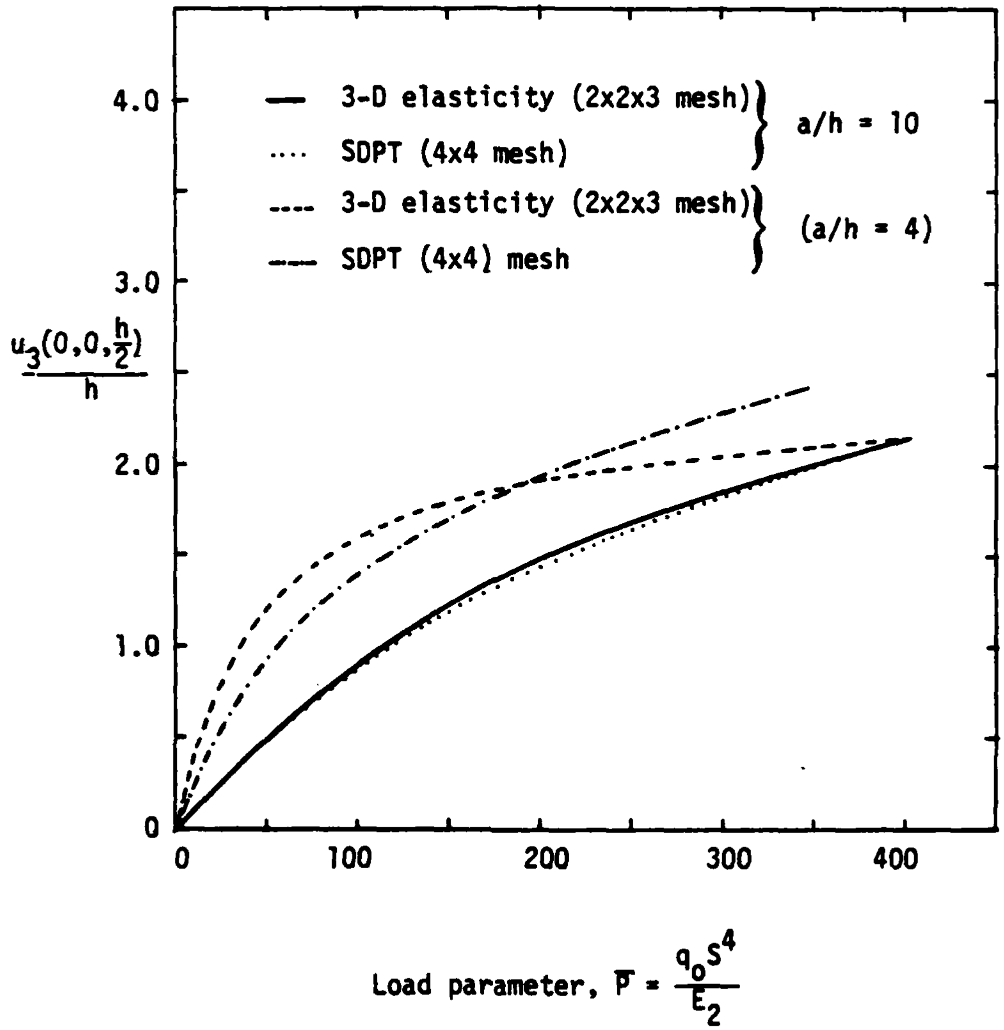


Figure 3 Load-deflection curves for cross-ply ($0^o/90^o/0^o$, equal thickness layers) square plates under uniformly distributed load ($E_1/E_2 = 25$, $G_{12} = G_{13} = 0.5E_2, G_{23} = 0.2\ E_2$, $\nu_{12} = 0.25$.

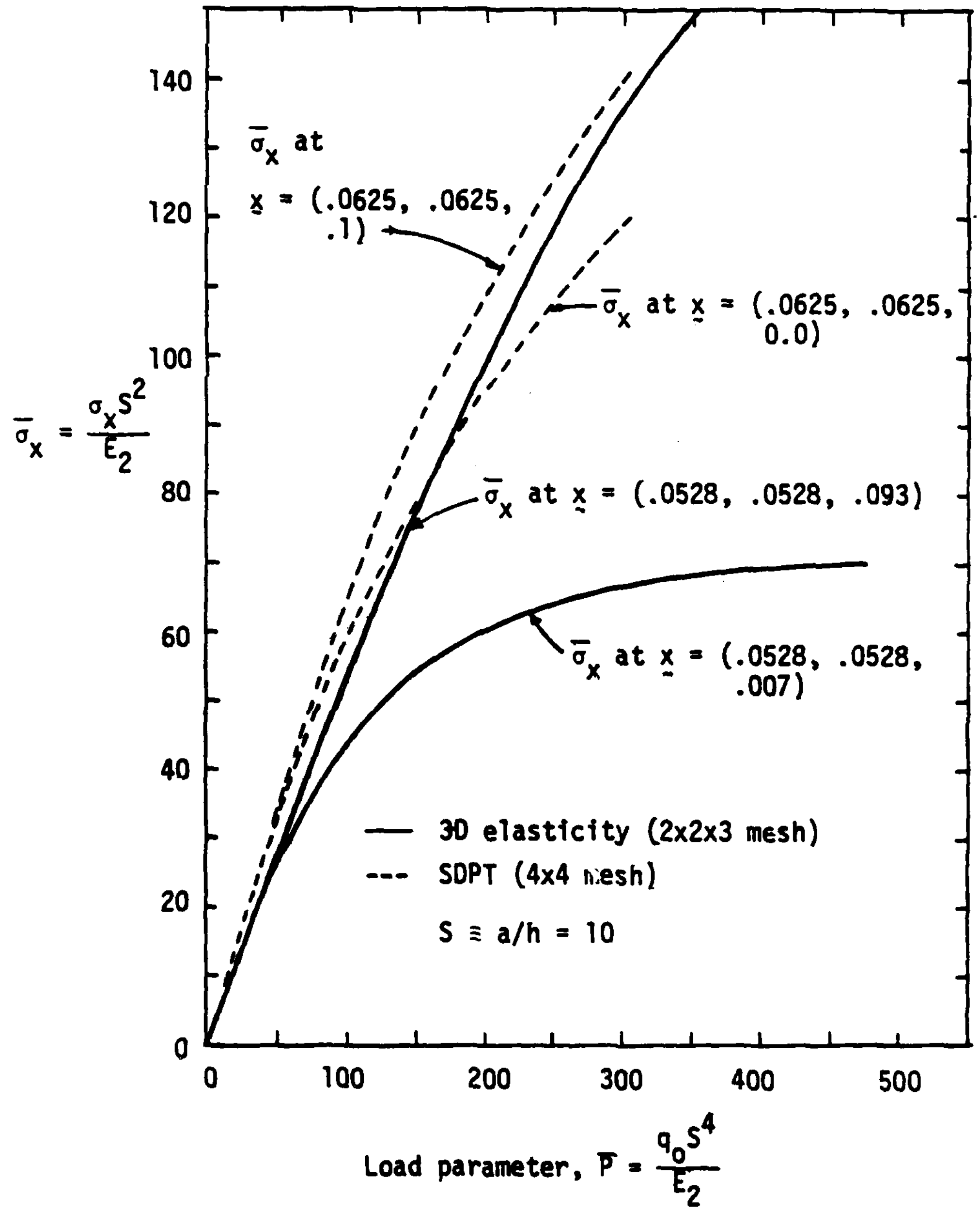


Figure 4 Normal stress versus load parameter for three-layer cross-ply (0°/90°/0°) square plate under uniform loading (S = a/h = 10).

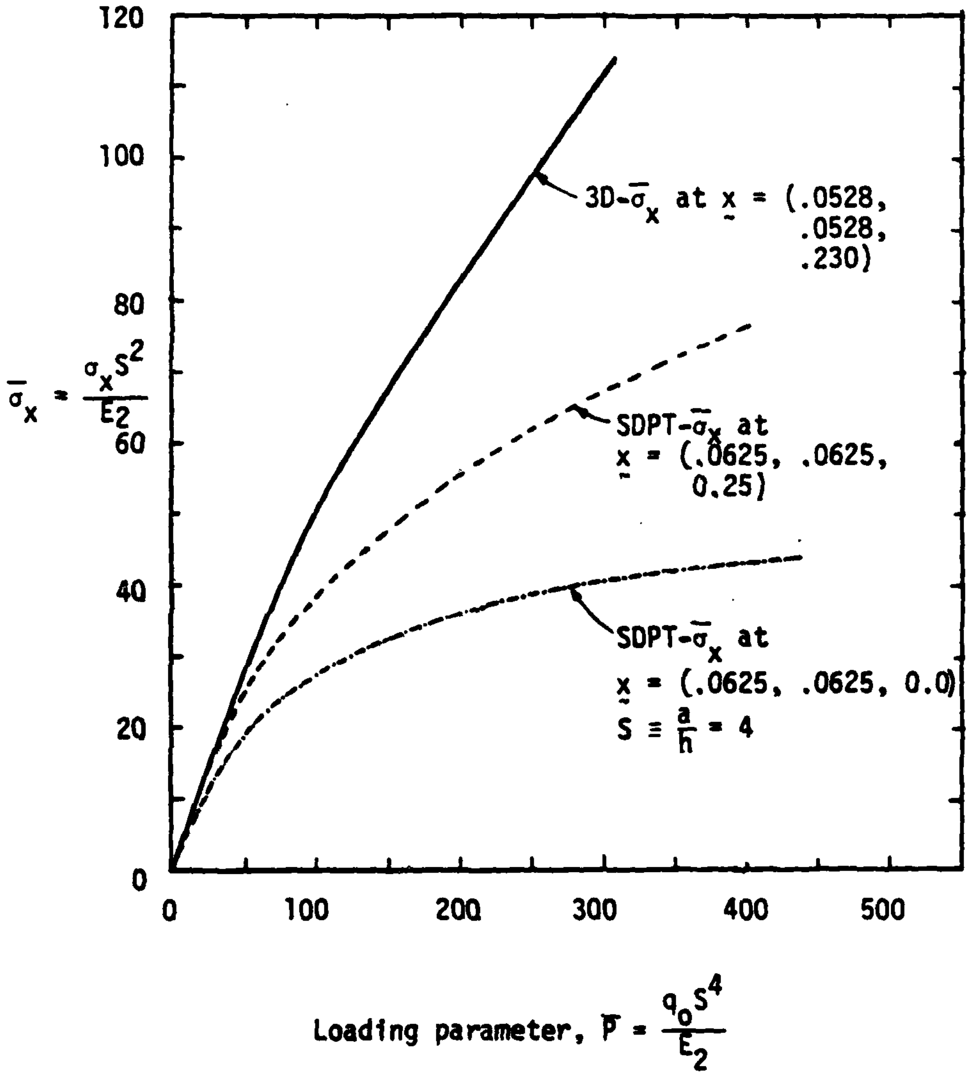


Figure 5 Center normal stress versus load parameter for three-layer cross-ply ($0^o/90^o/0^o$) square plate under uniform load ($S \equiv a/h = 4$).

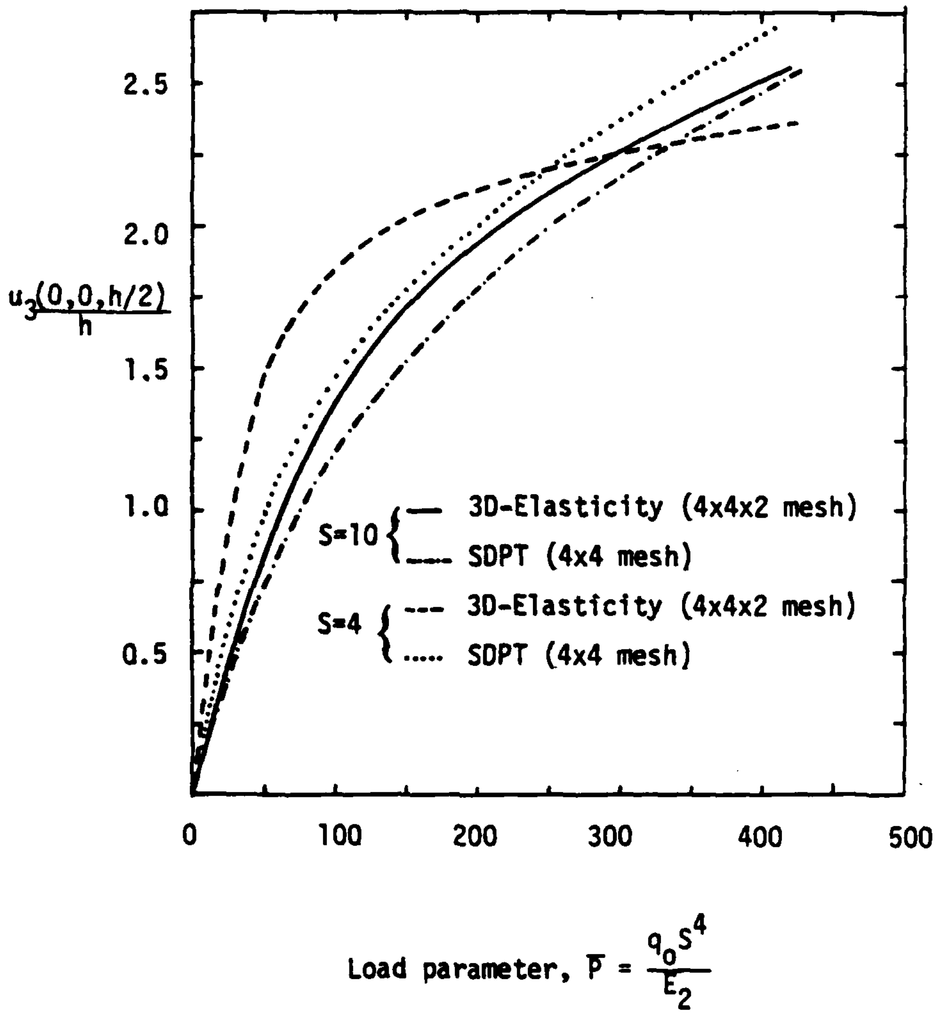


Figure 6 Load-deflection curves for two-layer, cross-ply ($0^o/90^o$) square plate under uniformly distributed load ($E_1 = 25E_2$, $G_{12} = G_{13} = 0.5E_2$, $G_{23} = 0.2E_2$, $\nu_{12} = 0.25$).

$$\bar{\sigma}_x = \frac{\sigma_x S^2}{E_2}$$

$$\bar{\sigma}_{xz} = \frac{\sigma_{xz} S}{E_2}$$

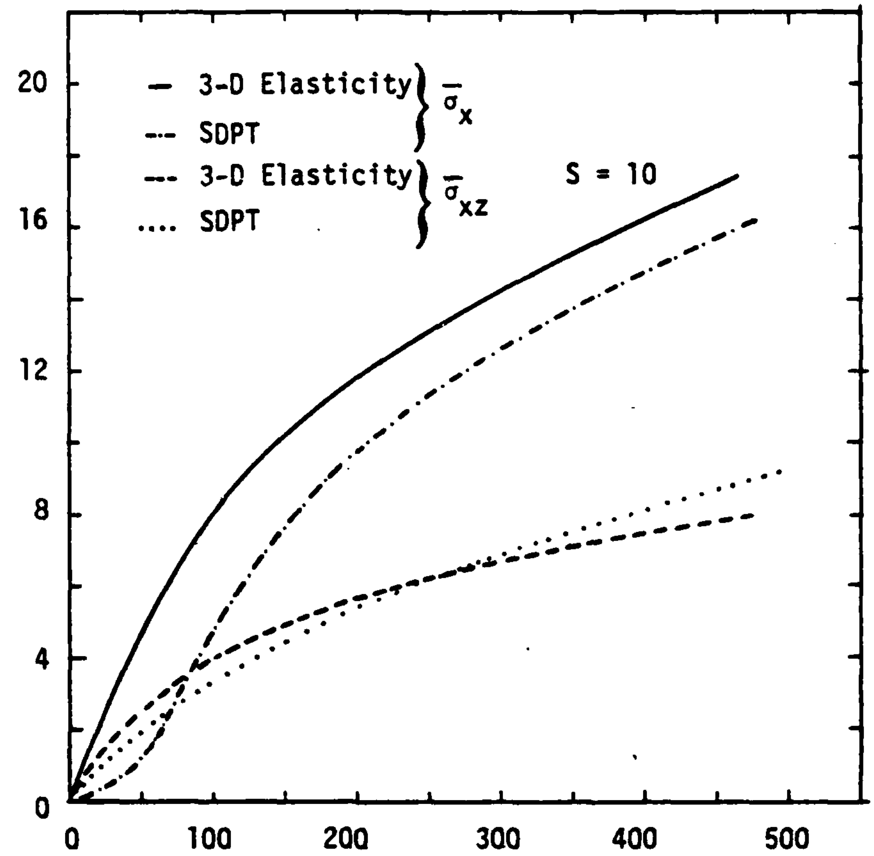


Load parameter, $\bar{P} = \frac{q_o S^4}{E_2}$

Figure 7 Normal and shear stresses versus load parameter for two-layer, cross-ply ($0^o/90^o$, S=10) square plate under uniformly distributed load ($\bar{\sigma}_x$ is computed at x = (.0625, .0625, 0.1) in SDPT; $\bar{\sigma}_{xz}$ is computed at x = (.4736, .4736, .0894) in 3D and at $\underset{\sim}{x}$ = (.4375, .4375, 0.1) in SDPT).

deflections and stresses can also be seen from Figs. 3-5. It should be noted that the plate theory solutions deviate more from the 3-D elasticity solutions as the thickness increases. Also, it should be pointed out that the stresses in the two theories are computed at different locations of the plate, and therefore part of the difference in the two solutions is attributable to the difference in the location of points at which the stresses are calculated.

Finally, a two-layer cross-ply (0°/90°) square plate under uniformly distributed load is analyzed and the plots of center deflection and stresses versus the load parameter are presented in Figs. 6 and 7. Note that the nonlinearity exhibited by the 3-D elasticity theory is less than that of the plate theory for load parameter values less than 250.

## 5. CONCLUSIONS

A finite-element analysis of geometrically nonlinear, three-dimensional theory of laminated plates is presented. It is found that the shear deformable plate theory results are fairly accurate when compared to the three-dimensional elasticity theory for side-to-thickness ratios of 10 or more. The difference between the two solutions is larger for a side-to-thickness ratio of 4. It is also found that the stresses predicted by the plate theory are in larger error than the deflections when compared to those predicted by the three-dimensional elasticity theory. The reduced integration technique is found to have an effect on the accuracy of the solution: reduced integration is recommended for thin plates ($a/h > 10$) and full integration for thick plates ($a/h < 10$), especially when geometric nonlinearities are included.

## Acknowledgments

The work reported herein is supported by the Structural Mechanics Section of NASA/Lewis and the Mechanics Division of the Office of Naval Research. The support is gratefully acknowledged.

REFERENCES

1. Reissner, E., and Stavsky, Y., "Bending and stretching of certain types of heterogeneous aerolotropic elastic plates," J. Appl. Mech., Vol. 28, 1961, pp. 402-408.

2. Yang, P. C., Norris, C. H., and Sta sky, Y., "Elastic wave propagation in heterogeneous plates," Int. J. Sol. Struct., Vol. 2, 1966, pp. 665-684.

3. Whitney, J. M., and Pagano, N. J., "Shear deformation in heterogeneous anisotropic plates," J. Appl. Mech., Vol. 37, 1970, pp. 1031-1036.

4. Reddy, J. N., and Chao, W. C., "A comparison of closed-form and finite element solutions of thick laminated anisotropic rectangular plates," Nuclear Engineering and Design, Vol. 64, 1981, pp. 153-167.

5. Reddy, J. N., "A penalty plate-bending element for the analysis of laminated anisotropic composite plates," Int. J. Num. Meth. Engng., Vol. 15, 1980, pp. 1187-1206.

6. Lo, K. H., Christensen, R. M., and Wu, E. M., "A higher-order theory of plate deformation: part 1, homogeneous plates; part 2, laminated plates," J. Appl. Mech., Vol. 44, 1977, pp. 663-668, 669-676.

7. Spilker, R. L., "High order three-dimensional hybrid-stress elements for thick-plate analysis," Int. J. of Num. Meth. in Engng., Vol. 17, 1981, pp. 53-69.

8. Pipes, R. B., and Pagano, N. J., "Interlaminar stresses in composite laminates under uniform axial extension," J. Composite Materials, Vol. 4, 1970, pp. 538-548.

9. Pipes, R. B., "Interlaminar stresses in composite laminates," AFML-TR-72-18, 1972.

10. Hsu, P. W., and Herakovich, C. T., "Edge effects in angle-ply composite laminates," J. Composite Materials, Vol. 11, 1977, pp. 422-428.

11. Lin, F. T., "The finite element analysis of laminated composites," Ph.D. Thesis, Virginia Polytechnic Institute and State University, December 1971.

12. Dana, J. R., "Three dimensional finite element analysis of thick laminated composites - including interlaminar and boundary effects near circular holes," Ph.D. Thesis, Virginia Polytechnic Institute and State University, August 1973.

13. Dana, J. R., and Barker, R. M., "Three dimensional analysis for the stress distribution near circular holes in laminated composites," Research report No. VPI-E-74-18, Virginia Polytechnic Institute and State University, August 1974.

14. Putcha, N. S. and Reddy, J. N., "Three-dimensional finite-element analysis of layered composite plates," Advances in Aerospace Structures, Winter Annual Meeting of ASME, Nov. 14-19, 1982, Phoenix, Arizona.

15. Pagano, N. J., "Exact solutions for rectangular bidirectional composites and sandwich plates," J. Composite Materials, Vol. 4, 1970, pp. 20-35.

16. Pagano, N. J. and Hatfield, S. J., "Elastic behavior of multilayered bidirectional composites," AIAA J., Vol. 10, 1972, pp. 931-933.

17. Jones, R. M., Mechanics of Composite Materials, McGraw-Hill, New York, 1975.

18. Reddy, J. N. and Rasmussen, M. L., Advanced Engineering Analysis, Wiley-Interscience, New York, 1982.

19. Haisler, W. E., Stricklin, J. S., and Stebbins, F. J., "Development and evaluation of solution procedures for geometric nonlinear analysis," AIAA J., Vol. 10, 1972, pp. 264-272.

20. Reddy, J. N. and Chao, W. C., "Non-linear bending of thick rectangular, laminated composite plates," Int. J. Non-Linear Mechanics, Vol. 16, 1981, pp. 291-301.

21. Levy, S., "Large deflection theory for rectangular plates," Proc. Symp. in Appl. Math., AMS, New York, Vol. 1, 1949, p. 197.

UNCLASSIFIED

SECURITY CLASSIFICATION OF THIS PAGE (When Data Entered)

# REPORT DOCUMENTATION PAGE

READ INSTRUCTIONS BEFORE COMPLETING FORM

| | |
|---|---|
| 1. REPORT NUMBER: VPI-E-82.31 | 2. GOVT ACCESSION NO.: AD-A124036 |
| 3. RECIPIENT'S CATALOG NUMBER | |
| 4. TITLE (and Subtitle): ANALYSIS OF LAYERED COMPOSITE PLATES BY THREE-DIMENSIONAL ELASTICITY THEORY | 5. TYPE OF REPORT & PERIOD COVERED: Interim |
| | 6. PERFORMING ORG. REPORT NUMBER: Tech. Report No. 31 |
| 7. AUTHOR(s): J. N. Reddy and T. Kuppusamy | 8. CONTRACT OR GRANT NUMBER(s): N00014-78-C-0647 |
| 9. PERFORMING ORGANIZATION NAME AND ADDRESS: University of Oklahoma, subcontracted to Virginia Polytechnic Institute | 10. PROGRAM ELEMENT, PROJECT, TASK AREA & WORK UNIT NUMBERS: NR 064-609 Mechanics Division |
| 11. CONTROLLING OFFICE NAME AND ADDRESS: Department of the Navy, Office of Naval Research Mechanics Division, Arlington, VA 22217 | 12. REPORT DATE: November, 1982 |
| | 13. NUMBER OF PAGES: 44 |
| 14. MONITORING AGENCY NAME & ADDRESS (if different from Controlling Office) | 15. SECURITY CLASS. (of this report): Unclassified |
| | 15a. DECLASSIFICATION/DOWNGRADING SCHEDULE |

16. DISTRIBUTION STATEMENT (of this Report)

This document has been approved for public release and sale; distribution unlimited.

17. DISTRIBUTION STATEMENT (of the abstract entered in Block 20, if different from Report)

18. SUPPLEMENTARY NOTES

The first part of the paper is submitted for presentation at 1983 ASME Vibrations Conference, Dearborn, Michigan. The second part is submitted to Computers and Structures journal.

19. KEY WORDS (Continue on reverse side if necessary and identify by block number)

composite materials, deflections, finite-element analysis, free vibrations, frequencies, geometrically nonlinear analysis, laminates, plates, stresses, three-dimensional theory of elasticity

20. ABSTRACT (Continue on reverse side if necessary and identify by block number)

The first part of the report is concerned with the natural vibrations of laminated plates, and the second part is concerned with geometrically nonlinear analysis of cross-ply laminates plates. A fully three-dimensional linear isoparametric element is used to determine natural frequencies, bending deflections and stresses.

DD FORM 1 JAN 73 1473 EDITION OF 1 NOV 65 IS OBSOLETE

UNCLASSIFIED

SECURITY CLASSIFICATION OF THIS PAGE (When Data Entered)